Journal of Biomedical Optics

SPIEDigitalLibrary.org/jbo

Simple and effective method for measuring translucency using edge loss: optimization of measurement conditions and applications for skin

Kenichiro Yoshida
Nobutoshi Komeda
Nobutoshi Ojima
Kayoko Iwata

SPIE

Simple and effective method for measuring translucency using edge loss: optimization of measurement conditions and applications for skin

Kenichiro Yoshida, Nobutoshi Komeda, Nobutoshi Ojima, and Kayoko Iwata
Kao Corporation, Beauty Research Center, 2-1-3 Bunka, Sumida Ward, Tokyo 131-8501, Japan

Abstract. We have developed a simple and effective method for everyday measurement of translucency with a handy spectral reflectometer using edge loss. Edge loss can be used to quantify the translucency index in terms of changes in reflectance under two types of measurement conditions. Here, a measurement condition represents the pairing of an illumination area and a measurement area. As a measure of the degree of lateral spread of reflected light, the translucency index can influence the appearance of human skin because this index represents eventual translucency. First, we estimated how edge loss changes when measurement conditions are varied. We then selected the combination of two measurement conditions of large and small edge loss to minimize errors. Finally, we estimated actual skin translucency changes before and after treatments comprising acetone-ether immersion and ultraviolet irradiation. The results were qualitatively consistent with the expectations under variations in absorbance and scattering capacity, indicating the effectiveness of this method in evaluating translucency. This method allows simultaneous measurement of translucency and reflectance as a spectrum, and also appears applicable for daily use, although common optical parameters cannot be derived using this method alone.
 [DOI: 10.1117/1.3646208]

Keywords: translucency; edge loss; spectral reflectometer; diffuse reflectance; skin tissue; target mask.

Paper 11076RRR received Feb. 27, 2011; revised manuscript received Aug. 4, 2011; accepted for publication Sep. 13, 2011; published online Oct. 28, 2011.

1 Introduction

Translucency is an important factor in giving skin a natural appearance and can also provide clues as to the internal condition of the skin. Given the importance of translucency, numerous studies have been performed on this parameter in the fields of medicine,[1–4] cosmetics,[5,6] and computer graphics.[7,8] In the field of cosmetics, one of the important goals is the improvement of skin appearance in daily life. In the field of medicine, the same can be said for cases where esthetic problems are a major concern. In such cases, the interest is in small variations in factors encountered during daily life (such as changes due to external stimuli like ultraviolet radiation, skin-care activities, or aging) as influences on appearance. The important issue is measuring translucency as an eventual lateral spread of reflected light and relating such measurements to appearance.

Most previous studies, however, have mainly discussed the standard optical properties of average human skin, with few studies attempting to assess individual differences or variations during daily life. Generally, translucency can be evaluated by calculating the absorption coefficient and effective scattering coefficient[3,8,9] or the effective attenuation coefficient[7,9] from a measured point spread function (PSF). One frequently used measurement configuration is the linear fiber array method, which involves a single optical fiber for light incidence and multiple optical fibers for light measurement lined up in a single row with the edges adjacent.[7,10] Another proposed configuration is video reflectometry measurement (VRM), which involves focusing light on the measurement surface through a system of lenses and using a camera to acquire images of the returning light.[3–5,8,11] Such conventional methods for translucency measurement need to detect weak signals from points adjacent to the incident point, thus requiring detection over a wide dynamic range and strict shielding from stray light from the environment and the incident point. In addition, given skin unevenness, point sources of light can be affected by the location of incidence. The instruments and protocols for measurement therefore tend to be elaborate to respond to these challenges.

Given this background, we tried to develop another method for easy detection of daily changes in translucency as the lateral spread of reflected light utilizing edge loss. Edge loss is a phenomenon known to cause changes in measurement values depending on the type of colorimeter.[12–14] Many studies have been conducted in the field of prosthetics, where the effect is particularly apparent and can easily result in esthetic issues.[12,14–18] Edge loss is also known to exert an influence when colorimetry is performed on human skin.[13] Studies of edge loss have shown that the choices of illumination area and measurement area exert major influences on the magnitude of colorimetry results.[12–14,16,17,19] Although some of these studies have suggested the idea of quantifying sample translucency using edge loss,[17,19] the choice of measurement conditions has not been adequately generalized.

We therefore began with a generalization of the relationship between illumination area, measurement area, and edge loss, and optimized the measurement conditions (the combination of illumination area and measurement area). We then evaluated

Address all correspondence to: Kenichiro Yoshida, Kao Corporation, Beauty Research Center, 2-1-3 Bunka, Sumida Ward, Tokyo 131-8501, Japan; Tel: +81-3-5630-9581; Fax: +81-3-5630-9341; E-mail: yoshida.kenichiro@kao.co.jp.

1083-3668/2011/16(11)/117003/8/$25.00 © 2011 SPIE

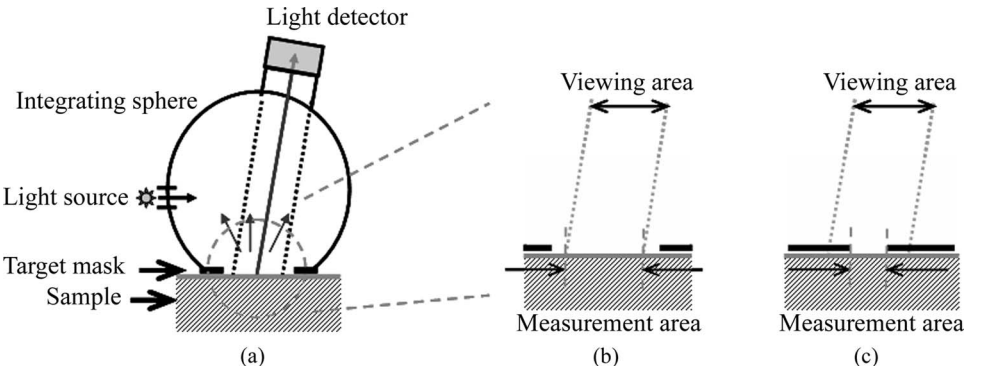

Fig. 1 (a) Schematic of the measurement device. Light from the light source is diffused by the integrating sphere and illuminates the sample. Part of the reflected light enters the detector and its spectrum is measured. (b) Measurement area when aperture radius exceeds detector viewing radius. The measurement radius is equal to the viewing radius. (c) Measurement area when detector viewing radius exceeds aperture radius. The measurement radius is equal to the aperture radius.

the adequacy of our optimization with translucent samples and examined how the translucency index varies with changes in the absorbing and scattering power of human skin.

2 Materials and Methods

2.1 *Measuring Device*

In our method, translucency is calculated from reflectances measured using a CM-2600d portable spectral reflectometer (Konica Minolta, Tokyo, Japan). This device has an optical system with diffusion light illumination/8-deg detection [Fig. 1(a)]. Reflectance can be measured in 10-nm increments across a 360–740-nm spectrum. Specular component excluded (SCE) mode was used in this study.

The CM-2600d reflectometer can alternate the detection radius between 4 and 1.5 mm, and the target mask that comes into contact with the sample can be changed. We utilized these features of the device in the present study. For normal measurements, a target mask with a 5.5-mm aperture radius is used when the detection radius is set to 4 mm (MAV mode), and a target mask with a 3-mm aperture radius is used when the detection radius is set to 1.5 mm (SAV mode). However, using a target mask with a different aperture radius allowed the creation of measurement conditions different from those normally used.

Let us consider how varying the aperture radius of the target mask changes the measurement radii when the detector viewing radius of the device is constant. If the viewing radius is smaller than the aperture radius, then the entire viewing area is the sample surface, and the measurement radius is equal to the viewing radius [Fig. 1(b)]. Conversely, if the viewing radius is larger than the aperture radius, then only the area of the sample within the aperture is exposed within the viewing area and the measurement radius is equal to the aperture radius [Fig. 1(c)].

2.2 *Formulation of Edge Loss*

To optimize the measurement conditions, we modeled reflectance measurement in order to evaluate edge loss for a given measurement conditions and a given PSF. Wavelength is not explicitly stated, but each parameter is in fact a function of wavelength. Using the bidirectional scattering surface reflectance distribution function (BSSRDF) $S(\vec{x}_\mathrm{i}, \vec{\omega}_\mathrm{i}; \vec{x}_\mathrm{o}, \vec{\omega}_\mathrm{o})$, incident radiance $L_\mathrm{i}(\vec{x}_\mathrm{i}, \vec{\omega}_\mathrm{i})$ from direction $\vec{\omega}_\mathrm{i}$ to point $\vec{x}_\mathrm{i}$ and outgoing radiance $L_\mathrm{o}(\vec{x}_\mathrm{o}, \vec{\omega}_\mathrm{o})$ from point $\vec{x}_\mathrm{o}$ in direction $\vec{\omega}_\mathrm{o}$ can be expressed according to the following relationship:[7,8]

$$L_\mathrm{o}(\vec{x}_\mathrm{o}, \vec{\omega}_\mathrm{o}) = \int_{A_\mathrm{i}} \int_{2\pi} S(\vec{x}_\mathrm{i}, \vec{\omega}_\mathrm{i}; \vec{x}_\mathrm{o}, \vec{\omega}_\mathrm{o}) \cdot L_\mathrm{i}(\vec{x}_\mathrm{i}, \vec{\omega}_\mathrm{i}) \cdot (\vec{n} \cdot \vec{\omega}_\mathrm{i})\, d\vec{\omega}_\mathrm{i} d\vec{x}_\mathrm{i}. \quad (1)$$

Here, $\vec{n}$ is the normal vector to the sample surface, and the integrated areas A_i and 2π are the illumination area and the solid angle of the hemisphere, respectively. Next, reflectance of the sample is expressed in terms of the outgoing radiance. Apparent reflectance can be written as r according to the following formula:

$$r = \frac{\int_{A_\mathrm{o}} L_\mathrm{os}(\vec{x}_\mathrm{o}, \vec{\omega}_\mathrm{d})\, d\vec{x}_\mathrm{o}}{\int_{A_\mathrm{o}} L_\mathrm{ow}(\vec{x}_\mathrm{o}, \vec{\omega}_\mathrm{d})\, d\vec{x}_\mathrm{o}}. \quad (2)$$

$L_\mathrm{os}(\vec{x}_\mathrm{o}, \vec{\omega}_\mathrm{d})$ and $L_\mathrm{ow}(\vec{x}_\mathrm{o}, \vec{\omega}_\mathrm{d})$ are the outgoing radiance in the direction of the detector of the sample and a standard white plate, respectively. Vector $\vec{\omega}_\mathrm{d}$ is the direction of the center of the detector as seen from the center of the measurement area, and the domain of integration A_o indicates the measurement area on the sample. Next, the BSSRDF of the sample $S_\mathrm{s}(\vec{x}_\mathrm{i}, \vec{\omega}_\mathrm{i}; \vec{x}_\mathrm{o}, \vec{\omega}_\mathrm{o})$ and the BSSRDF of the standard white plate $S_\mathrm{w}(\vec{x}_\mathrm{i}, \vec{\omega}_\mathrm{i}; \vec{x}_\mathrm{o}, \vec{\omega}_\mathrm{o})$ are related by the following formula:

$$\int_{2\pi} S_\mathrm{s}(\vec{x}_\mathrm{i}, \vec{\omega}_\mathrm{i}; \vec{x}_\mathrm{o}, \vec{\omega}_\mathrm{d}) \cdot L_\mathrm{i}(\vec{\omega}_\mathrm{i}) \cdot (\vec{n} \cdot \vec{\omega}_\mathrm{i})\, d\vec{\omega}_\mathrm{i} = R \cdot p(\vec{x}_\mathrm{i}, \vec{x}_\mathrm{o}) \cdot \int_{2\pi} S_\mathrm{w}(\vec{\omega}_\mathrm{i}; \vec{\omega}_\mathrm{d}) \cdot L_\mathrm{i}(\vec{\omega}_\mathrm{i}) \cdot (\vec{n} \cdot \vec{\omega}_\mathrm{i})\, d\vec{\omega}_\mathrm{i}. \quad (3)$$

However, $\int_{\vec{x}_\mathrm{o}} p(\vec{x}_\mathrm{i}, \vec{x}_\mathrm{o})\, d\vec{x}_\mathrm{o} = 1$ and $S_\mathrm{w}(\vec{\omega}_\mathrm{i}; \vec{\omega}_\mathrm{o}) = \int_A S_\mathrm{w}(\vec{x}_\mathrm{i}, \vec{\omega}_\mathrm{i}; \vec{x}_\mathrm{o}, \vec{\omega}_\mathrm{o}) d\vec{x}_\mathrm{o}$, where A is the whole surface. Here, we call R the true reflectance and $p(\vec{x}_\mathrm{i}, \vec{x}_\mathrm{o})$ the normalized PSF. $R \cdot p(\vec{x}_\mathrm{i}, \vec{x}_\mathrm{o})$ is the PSF weighted by incident radiance.

With further assumptions of isotropy and homogeneity regarding BSSRDF and incident radiance, Eqs. (1)–(3), apparent reflectance r can be calculated as follows:

$$r = \frac{R}{s} \cdot \int_{A_\mathrm{o}} \int_{A_\mathrm{i}} p(|\vec{x}_\mathrm{o} - \vec{x}_\mathrm{i}|)\, d\vec{x}_\mathrm{i} d\vec{x}_\mathrm{o}. \quad (4)$$

Here, s is the area of the sector $A_\mathrm{i} \cap A_\mathrm{o}$, and $p(\vec{x}_\mathrm{i}, \vec{x}_\mathrm{o})$ is replaced by $p(|\vec{x}_\mathrm{o} - \vec{x}_\mathrm{i}|)$.

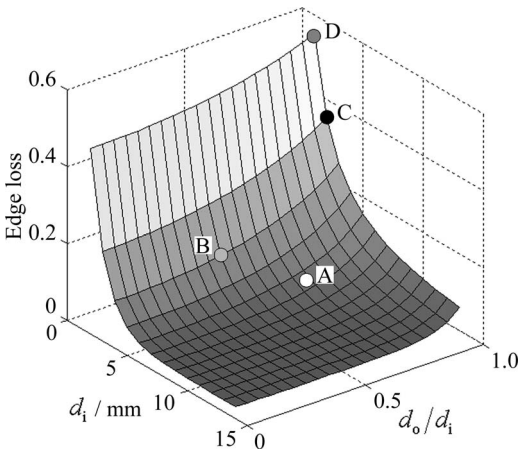

Fig. 2 Magnitude of edge loss for illumination radius (d_i) and measurement radius/illumination radius (d_o/d_i) given in Eq. (6) ($\mu_{eff} = 0.8\ mm^{-1}$) for normalized PSF. Points A–D in the plot show conditions used for reflectance measurement (see Table 1). Edge-loss values at points A–D in the plot were 0.050, 0.118, 0.354, and 0.553, respectively. The combination of A and C was used in Experiment 2.

Finally, edge loss is evaluated. When both the illumination radius and measurement radius are finite, apparent reflectance is less than true reflectance due to edge loss. We defined edge loss E quantitatively as this percentage decrease, as follows:

$$E = \frac{R - r}{R} = 1 - \frac{1}{s} \cdot \int_{A_o} \int_{A_i} p\left(|\vec{x}_o - \vec{x}_i|\right) d\vec{x}_i d\vec{x}_o. \quad (5)$$

2.3 *Optimization of Measurement Conditions*

From Eq. (5), we evaluated the relationship between illumination radius, measurement radius, and edge loss with numerical integration. Here we used a simple function system [Eq. (6)] as the function system for the PSF for the purpose of approximation because our objective was simply to evaluate the effect of the relative degree of lateral spread,

$$p\left(|\vec{x}_o - \vec{x}_i|\right) = \frac{\mu_{eff}}{2\pi} \cdot \frac{\exp\left(-\mu_{eff} \cdot |\vec{x}_o - \vec{x}_i|\right)}{|\vec{x}_o - \vec{x}_i|}. \quad (6)$$

Preliminary experiments showed that, using the red channel of the camera, the normalized PSF of human skin obtained by VRM[5,8] fit well with Eq. (6) if μ_{eff} was used as a fitting parameter. The mean value of μ_{eff} for Japanese forearm skin was around $0.8\ mm^{-1}$ (results of preliminary experiments, details not shown).

With numerical integration, changes in edge loss with the illumination radius d_i and the ratio of the measurement radius to the illumination radius d_o/d_i as parameters are evaluated. A plot of the results is shown in Fig. 2. Edge loss increases with decreasing d_i and increasing d_o/d_i. These results are consistent with findings from previous studies.[12–14,16,17]

Using the variation of edge loss under different conditions, the level of translucency of the sample can be evaluated. Selecting combinations so as to maximize the difference in edge loss facilitates detection of even small variations. Taking Fig. 2 as a reference, a good combination of conditions would be large d_i and small d_o/d_i together with small d_i and large d_o/d_i in order to maximize signal-to-noise ratio (S/N). Optimum conditions must be selected from among those possible, taking into account the additional restriction imposed by the device of possible viewing radii of 4 and 1.5 mm. In addition, radii that are too small will cause the measurement to be affected by the reduced amount of light reflected from the sample and by irregularities in skin topography and color unevenness.

Conditions A and C from Table 1 were ultimately selected as standard conditions to combine for calculating translucency index. Conditions B and D were used in experiment 1 for the purposes of comparison. The MAV mode was used for conditions A, C, and D, and the SAV mode was used for condition B. For conditions A and B, the standard target masks for the MAV and SAV modes were used, respectively. For conditions C and D, the aperture size of each target mask was customized by affixing a black sheet with a hole to a target mask for the MAV mode. Edge-loss values E(A), E(B), E(C), and E(D) in Fig. 2 were 0.050, 0.118, 0.354, and 0.553, respectively.

2.4 *Calculation of Reflectance and Translucency Index*

First, sample reflectance was recalculated from the device output values to exclude the reflected component from the target mask from measurement values. Apparent reflectance r_i under condition i is calculated from

$$r_i = \frac{r_{i,s} - r_{i,b}}{r_{i,w} - r_{i,b}}. \quad (7)$$

Here, $r_{i,w}$, $r_{i,b}$, and $r_{i,s}$ are the measured reflectance values of the standard white plate (a plastic plate supplied with

Table 1 Illumination radius (d_i) and measurement radius (d_o) conditions A–D and the respective geometrical settings.

	Measurement conditions			Geometrical settings (mm)			
Condition	d_i	d_o	d_o/d_i	Mode	Target mask	Viewing radius	Aperture radius
A	5.5	4	0.73	MAV	MAV (standard)	4	5.5
B	3	1.5	0.5	SAV	SAV (standard)	1.5	3
C	2	2	1	MAV	Customized	4	2
D	1	1	1	MAV	Customized	4	1

the spectral reflectometer; reflectance in the ordinary sense is 98.57 ± 0.29% at between 400 and 700 nm), blank, and the sample under condition i. Here, "blank" refers to the condition in which no light returns from the aperture. Reflectance calculated in this way represents the proportion of the amount of reflected light compared to that from the standard white plate. Basically, $r_{i,s}$ in this paper represents the mean value from five measurements.

Using the pair of apparent reflectances of the sample thus obtained under the combination of conditions i and j to meet $E(i) < E(j)$, the translucency index $T_{i,j}$ is defined by the following:

$$T_{i,j} = \frac{r_i - r_j}{r_i}. \tag{8}$$

From Eq. (5), it can be rewritten with edge loss as follows:

$$T_{i,j} = \frac{E(j) - E(i)}{1 - E(i)}. \tag{9}$$

From Eq. (9), it follows that when $E(i) \approx 0$, then $T_{i,j} \approx E(j)$. As can be seen from Fig. 2, within the possible extent of skin translucency, it is condition A that almost meets this condition. Hereafter, "translucency index" referred to by itself indicates $T_{A,C}$, and "reflectance" by itself refers to r_A.

2.5 *Experiments*

2.5.1 *Experiment 1: Preparation and measurement of translucent samples*

For the purpose of confirming the optimization, translucency indices of samples with different translucencies under multiple combinations (A/C, A/B, and C/D) were measured. Translucent samples were prepared as follows using transparent, room-temperature curing silicone resin (KE-108, condensed type; Shin-Etsu Silicones, Tokyo, Japan) as a base. A set amount of cosmetic foundation (in-house trial product) with similar color to average Japanese skin and catalyst (CAT-108; Shin-Etsu Silicones) was added to the KE-108, and the mixture was poured into a mold. Proportions of foundation-to-silicone resin were varied (0.05, 0.10, 0.15, 0.20, and 0.50 wt%) to adjust translucency. When the PSF of each sample was measured with VRM[5,8] and the μ_{eff} of the samples with foundation proportions of 0.05, 0.10, 0.15, 0.20, and 0.50 wt% was calculated according to Eq. (6), values came to 0.03, 0.24, 0.38, 0.63, and 1.38 mm^{-1} at the red channel, respectively (details not shown). Since μ_{eff} of forearm skin was ~0.8 mm^{-1} according to the results of our preliminary experiments, translucency of forearm skin in Japanese is expected to be between 0.20 and 0.50 wt%.

Values for r_A, r_B, r_C, and r_D of the translucent samples were calculated from Eq. (7), and $T_{A,C}$, $T_{A,B}$, and $T_{C,D}$ were then calculated from Eq. (8). Standard deviation for each translucency index $s_{T_{i,j}}$ was evaluated from standard deviations s_{r_i} for r_i and s_{r_j} for r_j by applying the error propagation equation to Eq. (8). S/N was evaluated by dividing the change in translucency index between different translucent samples by the error. As mentioned above, translucency of forearm skin in Japanese individuals is expected to be between 0.20 and 0.50 wt% at the red channel. Therefore, for each combined condition, S/N was regarded as the difference between translucency at 0.50 wt% and translucency at 0.20 wt% divided by the error for translucency at 0.20 wt% at 650 nm wavelength.

2.5.2 *Experiment 2: Measurement of human skin*

Experiment 2-1: A/E treatment. To examine the effect of scattering in the stratum corneum on translucency index, scattering power was varied by means of acetone-ether (A/E) treatment,[20] which dissolves lipid in the stratum corneum. The resulting reflectances and translucency indices were calculated. The inner forearms of adult males ($n = 6$) in their 30s and 40s were used. A total of five circular areas (2 cm i.d.) were selected on the left and right inner forearms, and these areas were immersed in an acetone-ether mixture for 30 min. Reflectances and translucency indices before and after treatment were measured.

Experiment 2-2: Ultraviolet-induced erythema. To consider the effect of accumulated pigment (hemoglobin) in the skin on reflectance and translucency index, the reflectance and translucency index of erythema induced by ultraviolet (UV) irradiation[21] were measured over time. The inner forearms of adult males ($n = 5$) in their 30s and 40s were used. One square area of sides 2 cm was irradiated for 10 min with UV radiation at a UV-B intensity of ~300 $\mu W/cm^2$ and a UV-A intensity of ~500 $\mu W/cm^2$. This dose is equivalent to approximately twice the minimal erythema dose in ordinary Japanese (result of preliminary experiments). The reflectance and translucency indices of the area exposed to UV radiation were measured before and one day after UV irradiation.

3 Results and Discussion

3.1 *Experiment 1: Measurement of Translucent Samples*

Reflectances were calculated from output values under each measurement condition using Eq. (7), and Fig. 3(a) shows translucency indices $T_{A,C}$, $T_{A,B}$, and $T_{C,D}$ at a wavelength of 650 nm and the errors calculated from these combinations with Eq. (8). Figure 3(b) shows the spectrum of translucency index $T_{A,C}$ as a representative example. The S/N designated in Sec. 2.5 was improved in the order of $T_{A,B}$, $T_{C,D}$, $T_{A,C}$ as 11.01, 15.08, 28.29, respectively.

This result supports the hypothesis set out in Sec. 2.3 that the S/N would improve with increasing change in edge loss. From the given edge loss values for conditions A-D in Fig. 2, changes in edge loss between combinations A-B, C-D, and A-C can be calculated as 0.068, 0.201, and 0.304, respectively, meaning that the ranking orders of changes in edge loss and S/N were consistent.

Looking at the comparative values of translucency indices between samples, for $T_{A,C}$ and $T_{A,B}$ the relationship was such that the index increased with increasing translucency across the whole range of sample translucencies. For $T_{C,D}$, however, this ranking order did not hold true between samples with higher translucency of ≤0.20 wt%.

The reason for this was considered to be that a considerable degree of edge loss occurs in condition i of Eq. (9) (condition C in this case). If translucency of the sample increases considerably, $E(j)$ approaches 1 and the variation of $E(j)$ becomes smaller. As a result, $E(j)$ becomes less sensitive than $E(i)$ in terms of translucency. As partially differentiating $T_{i,j}$ with respect to $E(i)$ in Eq. (9) always results in negative values, $T_{i,j}$ can be seen to decrease as $E(i)$ increases when $E(j)$ is constant. That is, if $E(i)$ increases significantly, $T_{i,j}$ will not necessarily

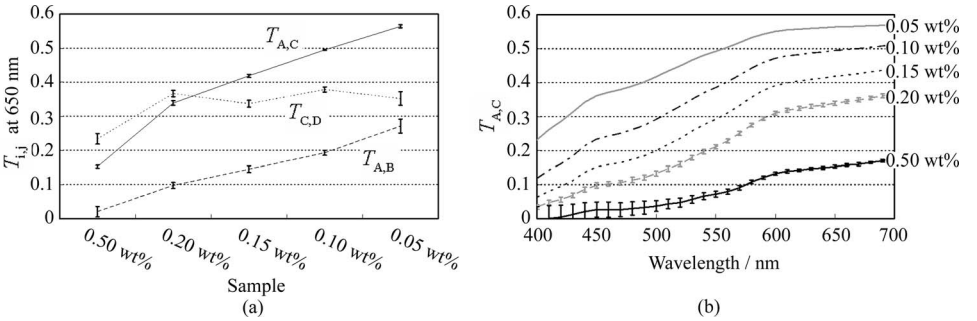

Fig. 3 (a) Translucency indices of prepared translucent samples (various combinations of measurement conditions for calculating translucency index) at a wavelength of 650 nm. The lower the concentration of foundation (measured in weight percent) in the sample, the higher the translucency. (b) $T_{A,C}$ as a representative example. Error bars are shown for 0.5 and 0.2 wt%. In order of increasing translucency, each line represents 0.50, 0.20, 0.15, 0.10, and 0.05 wt%, respectively.

increase despite increasing sample translucency. Taking these factors into account, it is particularly important to select condition i in Eq. (9) so that edge loss is minimized, in order to expand the coverage of translucency. This result also indicates that the selected combination, which is adequate for the measurement of skin translucency, may be inappropriate for objects with greater translucency.

3.2 *Experiment 2: Measurement of Human Skin*

Experiment 2-1: A/E treatment. Figure 4 shows average values for all subjects for reflectance and translucency index spectra before and after treatment for the areas treated with A/E. Reflectance increased after treatment, but the translucency index decreased. Here, values at a wavelength of 650 nm were extracted from the spectrum to specifically investigate the influence of changes in scattering power alone (Fig. 5). Reflectance and translucency index had changed significantly with a 99% confidence level.

These changes are reasonable from a qualitative perspective. The increase in the proportion of light reflected by the stratum corneum (where light absorption is weak) is considered to reduce the amount of light that reaches and returns from layers below this (where pigment absorb light), making reflectance increase. At the same time, light returning from shallow locations does not show much diffusion, with light diffusing more widely the deeper it reaches, making the translucency index decrease.

Experiment 2-2: UV-induced erythema. Figure 6 shows average values for all subjects for reflectance and translucency index spectra measured before and one day after treatment. Reflectance and translucency index were both decreased one day after treatment at a wavelength of ∼550 nm compared to before treatment. On the other hand, at ∼650 nm, reflectance was almost the same as before and the translucency index was increased. Figure 7 shows values at 550 and 650 nm extracted from the spectra. At 550 nm, both reflectance and translucency index values decreased significantly (99% confidence level). At 650 nm, reflectance was barely changed, but the translucency index was significantly increased (95% confidence level) after one day compared to before irradiation.

Changes at 550 nm are reasonable from a qualitative perspective. Reflectance decreased at a wavelength of 550 nm after one day as a result of erythema with a peak at 24–48 h.[21,22] Decreases in reflectance at a wavelength of 550 nm can be explained by the absorption spectrum of hemoglobin, which has strong peak at around 500–600 nm.[23,24] The fact that the translucency index also decreased can be explained by the depth reached by light and the degree to which this light contributes to diffusion. Hemoglobin present at a certain depth selectively absorbs the component of incident light that contributes to diffusion. Therefore, when reflectance decreases as a result of absorption by pigment, the translucency index also simultaneously decreases.

Although scattering power might also be changed in accordance with changes in thickness under conditions of erythema, the decrease in translucency index at 550 nm hardly seems to

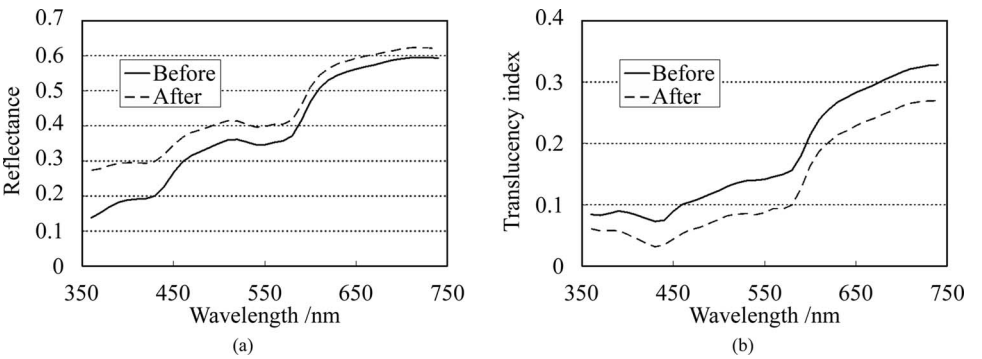

Fig. 4 Comparison before and after A/E treatment: (a) r_A and (b) $T_{A,C}$ spectrum. Solid lines: before treatment; dashed lines: after treatment. Values represent mean values for all subjects. r_A increased and $T_{A,C}$ decreased as a result of A/E treatment.

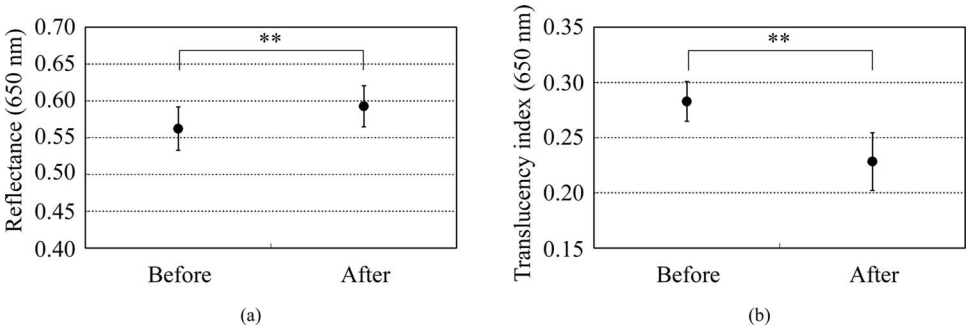

Fig. 5 Values at a wavelength of 650 nm extracted from spectra before and after A/E treatment: (a) r_A and (b) $T_{A,C}$. Significance was tested using a t-test (paired, bilateral). **: 99% confidence level.

be explained by variations in scattering power. Vascular dilation under conditions of erythema[22] can cause thickening of the skin and variations in scattering power. If we consider the fact that translucency was increased at 650 nm, at which the extinction coefficient of oxyhemoglobin is two orders of magnitude smaller[23] than the value at 550 nm and hemoglobin density has less effect on translucency than at 550 nm, scattering power should be changed in the direction of increasing translucency.

The order of the translucency index of skin and translucent samples using the proposed method are consistent with the order of μ_{eff} by VRM. From the results of Experiment 2, in which translucency index of skin was ~0.3 at 650 nm [Figs. 5(b) and 7(d)], and the result of Experiment 1, we can say that forearm skin in Japanese individuals shows a translucency between 0.20 and 0.50 wt%. The order of translucency is thus consistent with the order from VRM mentioned in Sec. 2.5.

Lastly, as an evaluation of the possibilities of the proposed method, absorption coefficients (μ_a) and effective scattering coefficients (μ_s') were roughly estimated from the reflectances (r_A) and translucency indices ($T_{A,C}$) of the result in Experiment 2. Given PSF as a function of the parameters μ_a and μ_s', and given specific values of each parameter, we can derive reflectance and translucency index with Eqs. (4)(8), substituting PSF into $R \cdot p\,(|\vec{x}_o - \vec{x}_i|)$. Inversely, μ_a and μ_s' can be derived from reflectance and the translucency index as an optimization problem. The formula proposed by Farrel et al.[2] was used as the PSF, as a function of μ_a, μ_s', refractive index, and the distance from the incident point. The refractive index was set at 1.3, as used by Jensen et al.[8] The parameters μ_a and μ_s' were calculated from r_A and $T_{A,C}$, using the "fminsearch" function in MATLAB software (Mathworks, Natick, Massachusetts), in which the Nelder–Mead simplex method is implemented, to solve the optimization problem.

The specific values of the results in Experiment 2 and the derived values of μ_a and μ_s' from these results are shown in Table 2. The large increases seen in μ_s' after A/E treatment (from 2.80 to 3.88) and in μ_a after UV-induced erythema (from 0.49 to 0.81) can be anticipated as natural results from changes in the skin. Each calculated μ_a and μ_s' at "before" at 650 nm and at 550 nm is generally larger (but not exceeding a tenfold increase) than the respective values at the red channel (for 650 nm) and green channel (for 550 nm) according to Jensen et al.[8] The differences are supposed to come not only from differences between subjects, but also from inadequate handling of standard white and surface reflection. We think that more appropriate treatment of these issues will increase the reliability of the derived optical properties.

3.3 *Limitations of this Measurement Method*

The limitations that we have identified thus far are as follows:

First, this method cannot deal with the anisotropy of translucency. Although a previous study showed that skin translucency is anisotropic,[10] the translucency index that this method derived represents the average over all directions. This method cannot deal with anisotropy due to the isotropic shape of the aperture.

A second issue is that the translucency of the standard white plate influences the translucency index values. In the proposed

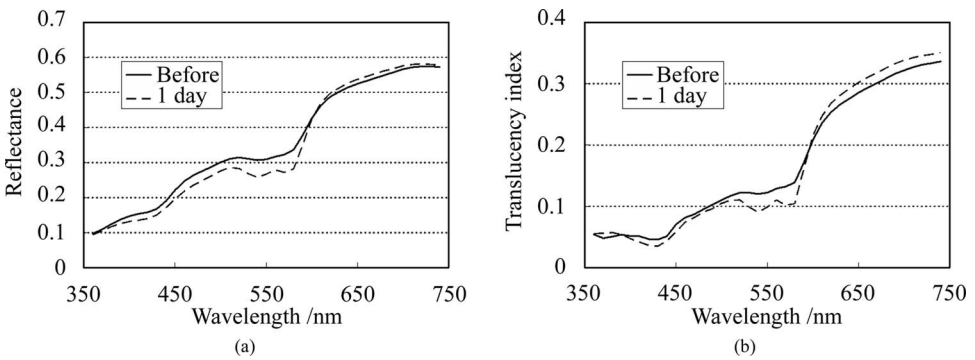

Fig. 6 Comparison of before and one day after UV irradiation: (a) r_A and (b) $T_{A,C}$. Solid lines: before irradiation; dashed lines: one day after irradiation. Values represent mean values for all subjects. Both r_A and $T_{A,C}$ decreased at a wavelength of ~550 nm after one day compared to before irradiation. On the other hand, $T_{A,C}$ increased while r_A was barely changed at 650 nm.

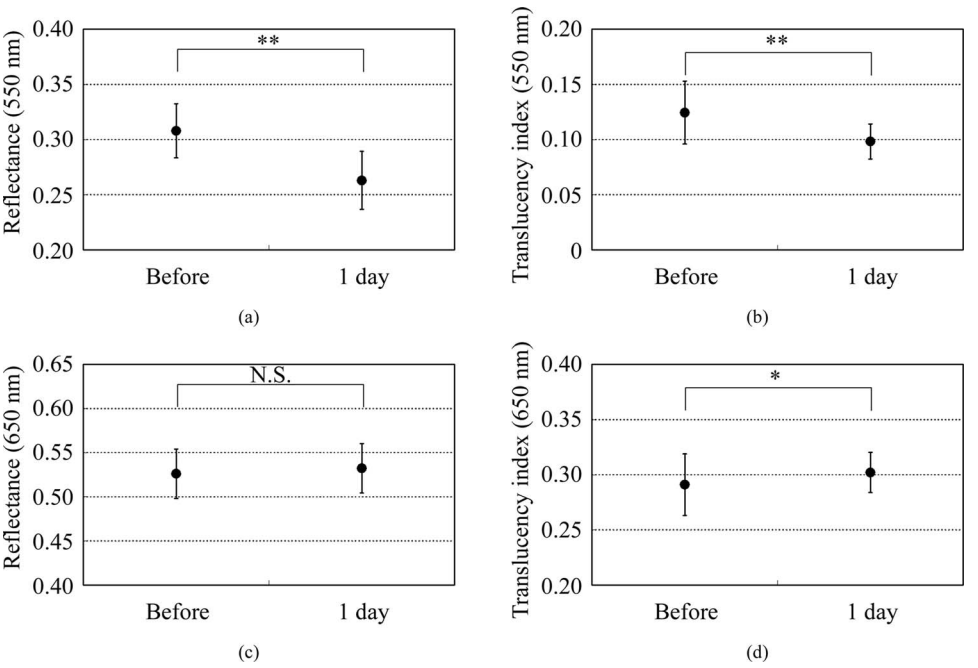

Fig. 7 Values at 550 and 650 nm extracted from spectra before and one day after UV irradiation: (a) r_A at 550 nm, (b) $T_{A,C}$ at 550 nm, (c) r_A at 650 nm, and (d) $T_{A,C}$ at 650 nm. Significance was tested using a t-test (paired, bilateral). **: 99% confidence level, *: 95% confidence level, N.S.: not significant.

method, the standard white plate is not only the standard for white, but is also the standard for opacity. When calculating reflectance according to Eq. (7), reflectance of the standard white plate is assumed to be constant even under different conditions. If the standard white plate is not completely opaque, however, reflectance will not be constant in the same way as for other translucent samples. If we want to obtain translucency indices of samples as absolute values or to compare indices of different instrument, then the opacity of the standard for white should be corrected.

The third point to consider is that surface reflection is not completely excluded in measurements. When gauging the internal condition of the skin, it is desirable to separate reflected light from the skin into surface reflection and inner reflection, and to calculate the degree of diffusion of inner reflection. Eliminating surface reflection would require adoption of a method such as polarization analysis.[25,26]

Table 2 Estimated values of μ_a and μ_s' from the results (r_A, $T_{A,C}$) in Experiment 2.

	Input		Output	
	r_A	$T_{A,C}$	μ_a/mm^{-1}	μ_s'/mm^{-1}
Experiment 2-1 (A/E treatment) at 650 nm				
Before	0.56	0.28	0.049	2.80
After	0.59	0.23	0.057	3.88
Experiment 2-2 (UV-induced erythema) at 550 nm				
Before	0.31	0.12	0.49	3.61
1 day	0.26	0.10	0.81	3.84

4 Conclusion

We have proposed a method for evaluating translucency by measuring reflectance under two different types of measurement conditions. Although the proposed method cannot lead to the determination of scattering and absorption coefficients by itself, translucency can be measured as a lateral spread, which was our aim, and some advantages appear to be offered over conventional methods. The signals to be detected in this method are the convolutions over the illumination and measurement areas, and are unlikely to be an order of magnitude smaller than the total amount of reflection. This method is thus expected to be less susceptible to the influence of stray light and skin unevenness. In addition, this method uses almost the same geometric condition as standard spectral reflectance measurement, allowing simultaneous measurement of translucency and reflectance. Furthermore, the translucency index can be measured as a spectrum that also provides useful information for detailed discussions, as we tried to consider the effect of scattering in Experiment 2-2. At present, in cases of skin appearance evaluation where eventual effects of translucency are of concern, this method can obtain sufficient information. If the values of the optical properties from the preliminary method we examined are related to those from conventional methods, then the method would be applicable as a practical tool for deriving these coefficients.

Acknowledgments

We express our gratitude to Takanori Igarashi for collaborating in the implementation of experiments during the initial

trial-and-error phase of this study, and to Koji Okubo and Takashi Kawata for providing extremely helpful support for the experiments involving A/E treatment and UV-induced erythema, respectively.

References

1. T. Nakai, G. Nishimura, K. Yamamoto, and M. Tamura, "Expression of optical diffusion coefficient in high-absorption turbid media," *Phys. Med. Biol.* **42**, 2541–2549 (1997).
2. T. J. Farrell, M. S. Patterson, and B. Wilson, "A diffusion theory model of spatially resolved, steady-state diffuse reflectance for the noninvasive determination of tissue optical properties *in vivo*," *Med. Phys.* **19**(4), 879–888 (1992).
3. S. L. Jacques, A. Gutsche, J. Schwartz, L. Wang, and F. K. Tittel, "Video reflectometry to extract optical properties of tissue *in vivo*," in *Medical Optical Tomography: Functional Imaging and Monitoring, IS11 of SPIE Institute Series*, pp. 211–226, SPIE Press, Bellingham, WA (1993).
4. L. Wang and S. L. Jacques, "Use of a laser beam with an oblique angle of incidence to measure the reduced scattering coefficient of a turbid medium," *Appl. Opt.* **34**(13), 2362–2366 (1995).
5. N. Komeda, N. Ojima, K. Okuzumi, J. Okada, K. Fukuda, and K. Hori, "Analysis of skin appearance based internal scattering of light," in *18th IFSCC Int. Conf. Proc.*, Florence, Italy, pp. 201–207 (2005).
6. A. Matsubara, "Skin translucency: what is it and how is it measured?" *24th IFSCC Congress Abstracts (Oral Session)*, Osaka, Japan, 92–93 (2006).
7. T. Weyrich, W. Matusik, H. Pfister, B. Bickel, C. Donner, C. Tu, J. McAndless, J. Lee, A. Ngan, H. W. Jensen, and M. Gross, "Analysis of human faces using a measurement-based skin reflectance model," *ACM Trans. Graphics (Proc. ACM SIGGRAPH 2006)* **25**(3), 1013–1024 (2006).
8. H. W. Jensen, S. R. Marschner, M. Levoy, and P. Hanrahan, "A practical model for subsurface light transport," *SIGGRAPH '01 Proc. of 28th Annual Conf. on Computer Graphics and Interactive Techniques*, 511–518 (2001).
9. W.-F. Cheong, S. A. Prahl, and A. J. Welch, "A review of the optical properties of biological tissues," *IEEE J. Quantum Electron.* **26**(12), 2166–2185 (1990).
10. S. Nickell, M. Hermann, M. Essenpreis, T. J. Farrell, U. Kramer, and M. S. Patterson, "Anisotropy of light propagation in human skin," *Phys. Med. Biol.* **45**, 2873–2886 (2000).
11. Z.-X. Jiang and P. D. Kaplan, "Point-spread imaging for measurement of skin translucency and scattering," *Skin. Res. Technol.* **14**, 293–297 (2008).
12. R. A. Bolt, J. J. ten Bosch, and J. C. Coops, "Influence of window size in small-window colour measurement, particularly of teeth," *Phys. Med. Biol.* **39**(7), 1133–1142 (1994).
13. H. Takiwaki, Y. Miyaoka, N. Skrebova, H. Kohno, and S. Arase, "Skin reflectance-spectra and colour-value dependency on measuring-head aperture area in ordinary reflectance spectrophotometry and tristimulus colourimetry," *Skin. Res. Technol.* **8**, 94–97 (2002).
14. Y.-K. Lee, B.-S. Lim, and C.-W. Kim, "Influence of illuminating and viewing aperture size on the color of dental resin composites," *Dent. Mater.* **20**, 116–123 (2004).
15. W. M. Johnston, N. S. Hesse, B. K. Davis, and R. R. Seghi, "Analysis of edge-losses in reflectance measurements of pigmented maxillofacial elastomer," *J. Dent. Res.* **75**(2), 752–760 (1996).
16. H. Yanagisawa, A. Ito, M. Nakamura, T. Ohyama, and A. Kobayashi, "Application of computer color matching for facial prosthetics, Part II: translucency of human skin and concentrations of pigments," *Gaku Ganmen Hotei (Maxillofacial Prosthet.)* **19**(1), 54–61 (1996). [in Japanese]
17. E. H. Rugh, W. M. Johnston, and N. S. Hesse, "The relationship between elastomer opacity, colorimeter beam size, and measured colorimetric response," *Int. J. Prosthodont.* **4**(6), 569–576 (1991).
18. J. T. Atkins and F. W. Billmeyer, Jr., "Edge-loss errors in reflectance and transmittance measurement of translucent materials," *Mater. Res. Stand.* **6**(11), 564–569 (1966).
19. Y.-K. Lee, H. Lu, and J. M. Powers, "Measurement of opalescence of resin composites," *Dent. Mater.* **21**, 1068–1074 (2005).
20. G. Imokawa, S. Akasaki, A. Kawamata, S. Yano, and N. Takaishi, "Water-retaining function in the stratum corneum and its recovery properties by synthetic pseudoceramides," *J. Soc. Cosmet. Chem.* **40**, 273–285 (1989).
21. W. Westerhof, O. Estevez-Uscanga, J. Meens, A. Kammeyer, and M. Durocq, "The relation between constitutional skin color and photosensitivity estimated from UV-induced erythema and pigmentation dose-response curves," *J. Invest. Dermatol.* **94**(6), 812–816 (1990).
22. G. J. Clydesdale, G. W. Dandie, and H. K. Muller, "Ultraviolet light induced injury: immunological and inflammatory effects," *Immunol. Cell. Biol.* **79**, 547–568 (2001).
23. R. R. Anderson and J. A. Parrish, "The optics of human skin," *J. Invest. Dermatol.* **77**, 13–19 (1981).
24. H. Takiwaki, "Measurement of erythema and melanin indices," Chapter 77 in *Handbook of Non-Invasive Methods and the Skin*, 2nd ed., pp. 665–671, CRC Press, Boca Raton (2006).
25. N. Ojima, S. Akazaki, K. Hori, N. Tsumura, and Y. Miyake, "Application of image-based skin chromophore analysis to cosmetics," *J. Imaging Sci. Technol.* **48**(3), 222–226, 236–238 (2004).
26. N. Tsumura, N. Ojima, K. Sato, M. Shiraishi, H. Shimizu, H. Nabeshima, S. Akazaki, K. Hori, and Y. Miyake, "Image-based skin color and texture analysis/synthesis by extracting hemoglobin and melanin information in the skin," *ACM Trans. Graphics (Proc. ACM SIGGRAPH 2003)* **22**(3), 770–779 (2003).